

Picosecond primary structural transition of the heme is retarded after nitric oxide binding to heme proteins

Sergei G. Kruglik^{a,b,1}, Byung-Kuk Yoo^a, Stefan Franzen^c, Marten H. Vos^a, Jean-Louis Martin^a, and Michel Negre^{a,1}

^aLaboratoire d'Optique et Biosciences, Institut National de la Santé et de la Recherche Médicale, Ecole Polytechnique, 91128 Palaiseau, France;

^bLaboratoire Acides Nucléiques et Biophotonique, Université Pierre et Marie Curie, 75252 Paris, France; and ^cDepartment of Chemistry, North Carolina State University, Raleigh, NC 27695

Edited by Robin M. Hochstrasser, University of Pennsylvania, Philadelphia, PA, and approved June 23, 2010 (received for review November 9, 2009)

We investigated the ultrafast structural transitions of the heme induced by nitric oxide (NO) binding for several heme proteins by subpicosecond time-resolved resonance Raman and femtosecond transient absorption spectroscopy. We probed the heme iron motion by the evolution of the iron-histidine Raman band intensity after NO photolysis. Unexpectedly, we found that the heme response and iron motion do not follow the kinetics of NO rebinding. Whereas NO dissociation induces quasi-instantaneous iron motion and heme doming (<0.6 ps), the reverse process results in a much slower picosecond movement of the iron toward the planar heme configuration after NO binding. The time constant for this primary domed-to-planar heme transition varies among proteins (~30 ps for myoglobin and its H64V mutant, ~15 ps for hemoglobin, ~7 ps for dehaloperoxidase, and ~6 ps for cytochrome c) and depends upon constraints exerted by the protein structure on the heme cofactor. This observed phenomenon constitutes the primary structural transition in heme proteins induced by NO binding.

time-resolved Raman spectroscopy | allostery | structural dynamics

The role of diatomics endogenously generated in cells as messengers in various signaling pathways has been demonstrated for nitric oxide (NO) (1, 2) and carbon monoxide (CO) (3, 4) and various gas-sensors heme proteins have been discovered in the last two decades (5). In these signaling pathways, the binding of diatomics to their respective heme sensor domain triggers a response of the associated enzymatic domain by modulating the catalytic or the gene regulating activity (5). Recently, myoglobin (Mb) was proposed to be involved in the regulation of NO level (6), and neuroglobin was proposed as a sensor regulating the NO/O₂ balance (7). Similarly to Hb (8–10), the signaling mechanisms are based at the molecular level on an allosteric structural change of the receptor/sensor protein coupled to a change of activity or affinity and are induced by diatomic ligation to the heme iron cofactor. The signal of diatomic binding/release can be transmitted to the overall protein structure either by in-plane/out-of-plane motion of the iron through the bound proximal histidine or by the cleavage of the iron-histidine (Fe-His) bond. In particular, for Hb and its monomeric counterpart Mb, the out-of-plane iron motion occurs in less than 1 ps after gaseous ligand release (11, 12) and represents the first event of the allosteric R → T transition (9). This primary heme iron motion is followed by overall tertiary changes, notably motion of α -helices (13). Upon gaseous ligand binding, the reverse T → R allosteric transition is coupled to the iron motion toward the heme plane, and this primary motion is also considered quasi-instantaneous since the stereochemical description of Hb allostery by Perutz (9, 10) although up to now it has never been observed.

The ultrafast events in the interaction of heme proteins with various gaseous ligands were studied extensively at molecular level in the last two decades by femtosecond transient absorption (TA) (14, 15) and time-resolved IR (TR-IR) (16, 17) spectroscopies. Time-resolved resonance Raman (18, 19) (TR³) and X-ray

diffraction (TRXD) (20–23), two structure-sensitive techniques able to probe the heme iron position, focused so far on the heme-CO complex, studying the consequences of CO release. At the same time, the binding of a diatomic and subsequent T → R transition have not yet been studied by a time-resolved technique sensitive to heme structural changes. The first event following gaseous ligand binding, namely, the transition from domed-to-planar heme, is believed to occur in less than 0.6 ps, by analogy with the well-studied heme response to ligand release (11, 12, 24, 25), although the structural constraints and energy barriers for these two opposite processes are not necessarily the same.

We investigated the primary event related to the T → R transition by subpicosecond TR³ and report the observation of the in-plane movement of the ferrous heme iron induced by NO geminate rebinding, following a femtosecond photodissociating laser pulse. We studied various nitrosylated heme proteins: wild-type Mb and its distal mutant H64V, Hb, and dehaloperoxidase (DHP), all incorporating a *b*-type heme, and mitochondrial cytochrome *c* (Cyt *c*) having a *c*-type heme covalently linked to the protein. This allowed the evaluation of distinct structural parameters that could influence the iron motion. The conformational transition between domed and planar heme structure was monitored in TR³ spectra of the photoproduct through temporal evolution of the intensity of Fe-His stretching (26) ($\nu_{\text{Fe-His}}$), an important vibrational mode linking heme iron with the proximal histidine that transmits the binding information to the protein structure. Our approach is based on the findings that (i) the transition from planar to domed heme structure induces a change in Raman intensity of the low-frequency $\nu_{\text{Fe-His}}$ stretching band (19, 26) located within the range 200–240 cm⁻¹; (ii) the intensity of $\nu_{\text{Fe-His}}$ resonantly excited within the Soret absorption band depends on the out-of-plane position of the iron with respect to the heme macrocycle plane (27) and is zero for the in-plane iron position. For this study, we have employed a specially designed home-built subpicosecond TR³ spectrometer having ~0.7-ps temporal and ~25-cm⁻¹ spectral resolution (24, 28, 29), probing structural changes in the time range not yet accessible to TRXD.

Results

Difference Between Iron Motion and Dynamics of NO Binding. The TR³ spectra of ferrous Mb-NO in the low-frequency range of Fe-His mode at various time delays after NO photodissociation are presented in Fig. 1A. The Raman spectrum of five-coordinate

Author contributions: S.G.K., M.H.V., J.-L.M., and M.N. designed research; S.G.K., B.-K.Y., and M.N. performed research; S.F. contributed new reagents/analytic tools; S.G.K., B.-K.Y., S.F., M.H.V., and M.N. analyzed data; and S.G.K., M.H.V., J.-L.M., and M.N. wrote the paper.

The authors declare no conflict of interest.

This article is a PNAS Direct Submission.

¹To whom correspondence should be addressed. E-mail: michel.negre@polytechnique.fr or sergei.kruglik@upmc.fr.

This article contains supporting information online at www.pnas.org/lookup/suppl/doi:10.1073/pnas.0912938107/-DCSupplemental.

deoxy Mb possessing a domed heme is dominated by $\nu_{\text{Fe-His}}$ at 219 cm^{-1} . The spectrum of the ground-state nitrosylated complex recorded at negative time delay between the photolysis and Raman probe pulses ($\Delta t = -5 \text{ ps}$) does not exhibit the $\nu_{\text{Fe-His}}$ mode, as expected for a six-coordinate planar heme. After the femtosecond photolysis pulse, $\nu_{\text{Fe-His}}$ appears already at $\Delta t = 1 \text{ ps}$ with high intensity due to NO dissociation and immediate out-of-plane motion of the iron toward proximal His, forming a domed heme. We emphasize that, because the difference TR³ spectra at positive delay in Fig. 1A originate solely from the photoproduct species (see *Materials and Methods*), the intensity decay kinetics of $\nu_{\text{Fe-His}}$ (Fig. 1B) directly reflects the evolution of the photoproduct structure.

The striking feature of this kinetics is that the intensity of the mode $\nu_{\text{Fe-His}}$ (which is located at 225 cm^{-1} at $\Delta t = 2 \text{ ps}$ and gradually shifts to $\sim 222 \text{ cm}^{-1}$ at $\Delta t = 100 \text{ ps}$) remains nearly constant during the first 10 ps, contrary to absorption kinetics. Indeed, it is established from visible TA experiments on Mb-NO (Table 1 and Fig. S1; refs. 15 and 29) that about 40%

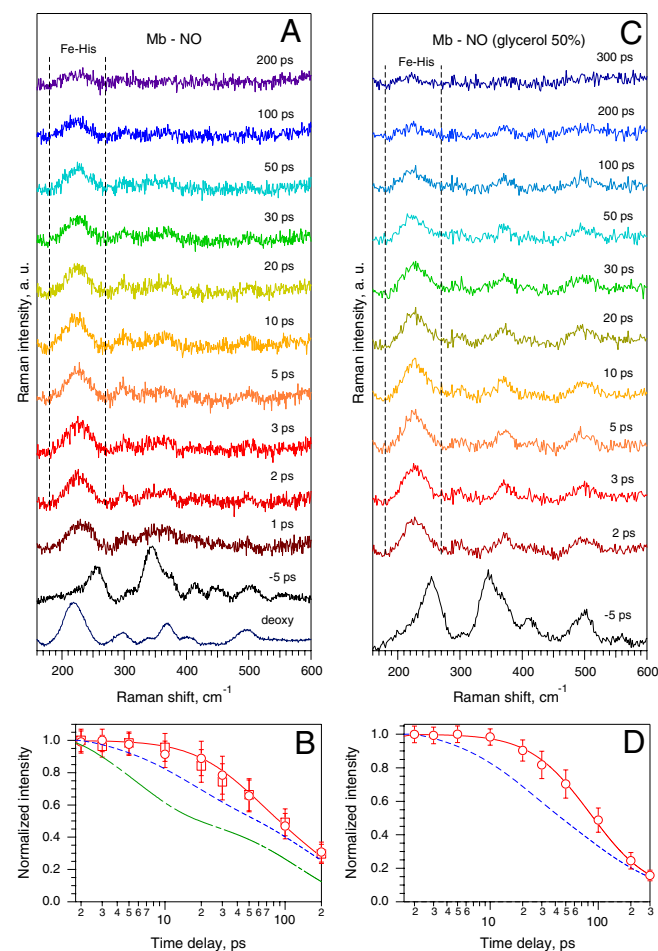


Fig. 1. TR³ spectra of ferrous Mb in interaction with NO and kinetics of the $\nu_{\text{Fe-His}}$ mode. (A) Ground-state Raman spectra of deoxy Mb and of six-coordinate NO-liganded Mb (-5 ps), and difference TR³ spectra after NO photodissociation at indicated time delays after photolysis. (B) Evolution of normalized area of the $\nu_{\text{Fe-His}}$ mode contour ($180\text{--}270 \text{ cm}^{-1}$), between the vertical dotted lines in A for two Mb concentrations: 0.3 mM (circles) and 0.1 mM (squares). The red curve is the solution of rate equations for population decay of all nonplanar heme species, yielding the time of transition from domed-to-planar 6-c heme $\tau_D = 30 \pm 10 \text{ ps}$. The blue and green dashed curves are, respectively, double-exponential decays after NO dissociation from transient visible (Table 1) and from IR absorption ($\tau_1 = 5.3 \text{ ps}$ [54%], $\tau_2 = 133 \text{ ps}$ [46%]; ref. 17). (C and D) The same for Mb-NO in 50% glycerol solution, yielding $\tau_D = 40 \pm 15 \text{ ps}$.

of five-coordinate heme population converts into the six-coordinate form with time constant of $\sim 10 \text{ ps}$, followed by a second geminate phase in $\sim 150 \text{ ps}$. Moreover, TR-IR measurements (17) of the stretch of bound NO in Mb-NO have shown that $\sim 54\%$ of NO rebinds to the iron with time constant of 5.3 ps. Remarkably, the decay of the $\nu_{\text{Fe-His}}$ intensity compared with those of transient visible and IR absorption (Fig. 1B) is obviously different and much slower.

Several phenomena could influence this unexpected $\nu_{\text{Fe-His}}$ intensity kinetics. First, the accurate measurement of $\nu_{\text{Fe-His}}$ intensity could be perturbed by reabsorption of scattered Raman light. However, sample illumination from the bottom of the cell near the inner surface has been specially designed in order to minimize this effect. Indeed, this possibility was ruled out by the observation that the $\nu_{\text{Fe-His}}$ intensity kinetics for two different Mb concentrations (0.1 mM and 0.3 mM) exhibit exactly the same behavior (Fig. 1B). Second, the intensity of $\nu_{\text{Fe-His}}$ depends not only on the population of the domed heme species but also on Raman resonance enhancement, so that time-dependent spectral shift of transient absorption may influence the result (30), along with the process of vibrational relaxation (28). However, these effects vanish in a few picoseconds, and therefore the kinetics of $\nu_{\text{Fe-His}}$ was analyzed in the time range $\Delta t = 2\text{--}200 \text{ ps}$, where TA spectra of Mb-NO show a clear isosbestic point (Fig. S1).

After having discarded these possible artifacts, because the intensity of $\nu_{\text{Fe-His}}$ resonantly excited in the Soret absorption band depends on the out-of-plane position of the iron with respect to the heme plane (27; *SI Text*), we conclude that the kinetics of $\nu_{\text{Fe-His}}$ intensity (Fig. 1B) directly represents the transition from domed-to-planar heme structure and consequently the movement of the iron triggered by NO binding. Thus, the $\nu_{\text{Fe-His}}$ intensity decay would be identical to the kinetics measured by TA or TR-IR if the iron were moving instantaneously upon NO binding, which is not the case. Accordingly, because the parameters probed by TA/TR-IR and TR³ are not the same (NO coordination to the iron versus heme iron position), we interpret our observation as follows: The photolyzed NO molecules from the heme pocket bind to the iron of the domed five-coordinate heme and the resulting transient six-coordinate heme complex does not return immediately to a planar configuration, but remains domed for some time, providing enhancement for the $\nu_{\text{Fe-His}}$ Raman intensity.

To analyze quantitatively this effect, the evolution of $\nu_{\text{Fe-His}}$ intensity has been fitted by the convolution of Raman instrumental response function with the solution of rate equation (Eq. 1) for population changes of all nonplanar heme species (see *Materials and Methods*). We employed a kinetic model of NO recombination (Fig. 2A) based on TA measurements (15, 29) (Fig. S1) incorporating an additional transient six-coordinate species with nonplanar structure, not detected by TA as a separate component (Table 1). In Raman spectra ($\Delta t = 1\text{--}200 \text{ ps}$) of Fig. 1A the intensity of the $\nu_{\text{Fe-His}}$ band originates from two different domed species: the photodissociated five-coordinate domed heme (5c-His; species X, B, and *Const.* in Fig. 2A) and six-coordinate NO-liganded domed heme (6c-His-NO; species D), which can exist only transiently. The solid red curve through the data points in Fig. 1B is the best-fit kinetics yielding the time constant $\tau_D = 30 \pm 10 \text{ ps}$ for the domed-to-planar heme transition (D \rightarrow A) using the TA time constants in Table 1. This picosecond heme iron motion represents the first structural event in wild-type Mb taking place after NO binding.

Other Experimental Evidence for the Transient Population of Domed Six-Coordinate Heme. It is essential to compare the behavior of $\nu_{\text{Fe-His}}$ to that of the ν_4 band, which is a π electron density marker also sensitive to spin and coordination state of the heme iron (31). Therefore, in another experiment we recorded simultaneously (with a less dispersive spectrograph grating) the temporal changes of the modes $\nu_{\text{Fe-His}}$ and ν_4 (Fig. 3 and Figs. S2 and S3).

Table 1. Kinetic parameters obtained from transient absorption measurements and fitting the $\nu_{\text{Fe-His}}$ Raman intensity kinetics (τ_D)

Protein	NO rebinding phases (from transient absorption)			Heme iron motion τ_D (from $\nu_{\text{Fe-His}}$ kinetics)
	τ_1 (amplitude)	τ_2 (amplitude)	Constant	
Myoglobin	13 ps (0.40)	148 ps (0.50)	0.10	30 ± 10 ps
Myoglobin in 50% glycerol	15.3 ps (0.42)	71 ps (0.36) $\tau_3 = 378$ ps (0.21)	0.01	40 ± 15 ps
Myoglobin H64V mutant	10 ps (0.51)	92 ps (0.43)	0.06	30 ± 15 ps
Dehaloperoxidase	14 ps (0.61)	65 ps (0.38)	0.01	7 ± 2 ps
Cytochrome c	8.4 ps (0.99)	—	0.01	6 ± 2 ps
Hemoglobin	10.8 ps (0.74)	61 ps (0.22)	0.04	15 ± 6 ps

Only for Mb in 50% glycerol, we found a third component.

A straightforward separation of the mode ν_4 corresponding specifically to species D is rather complicated by the facts that (i) the frequency difference between the limiting values for six-coordinate planar Mb-NO ($1,374 \text{ cm}^{-1}$) and five-coordinate domed deoxy-Mb ($1,354 \text{ cm}^{-1}$) is 20 cm^{-1} (Fig. 3), whereas our spectral resolution is 25 cm^{-1} ; (ii) because the ν_4 band position is sensitive to polar heme environment, we may expect fine ν_4 -frequency difference between the species X (NO far from the heme) and B (NO in the vicinity of the heme), so that four different components (or a continuous distribution) are expected to contribute to the resulting Raman contour; (iii) in our experiments the total amount of the photoproduct species constitutes no more than 35% (determined by ground-state subtraction) of the probed molecules and from this amount, the maximal population of species D is about 24% (Fig. 2B).

Therefore, we compared the photoproduct transient spectra at various time delays with that at 2 ps (minimal contribution of species D). The spectrum at 30 ps with maximal contribution

of D (Fig. 2C) is highlighted in Fig. 3. Importantly, the intensity of the ν_4 band ($1,355 \text{ cm}^{-1}$) clearly decreased at 30 ps, whereas that of $\nu_{\text{Fe-His}}$ intensity is much less pronounced (Fig. 3). The difference (Fig. 3E) reveals a pronounced high-frequency shift of the ν_4 band (shift centered at $\sim 1,362 \text{ cm}^{-1}$), whereas the bands ν_7 ($672\text{--}675 \text{ cm}^{-1}$) and $\nu_{\text{Fe-His}}$ ($223\text{--}225 \text{ cm}^{-1}$) experience only very small shifts. Fig. S3 shows transient spectra in the entire frequency range and difference traces with ν_4 band shift for all time delays. Fig. S4 shows that the kinetics of band ν_4 is well superimposed with the TA decay and not with that of $\nu_{\text{Fe-His}}$, within the accuracy of measurements. We thus conclude that the intensity of the band ν_4 follows heme coordination, whereas that of the $\nu_{\text{Fe-His}}$ band does not.

Increasing the viscosity of the solvent enhances the yield and rates of geminate rebinding and can slow down the structural protein relaxation (15, 32). We thus also performed TR³ measurements for Mb-NO in 50% glycerol solution (Fig. 1C) in order to investigate a change of τ_D for Mb as a function of viscosity. We found that the corresponding TA kinetics were best fitted with a triple-exponential (Table 1) and best-fit analysis of TR³ data using modified rate equations yielded $\tau_D = 40 \pm 15$ ps (Fig. 1D)

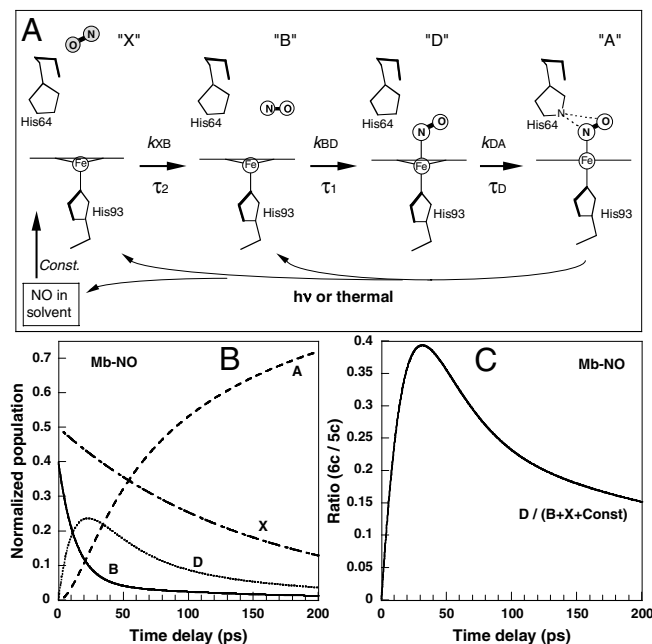


Fig. 2. Scheme of NO recombination to Mb together with relevant transient species within the picosecond time range (A). The positions of His side chains are obtained from structures (2FRK and 2V1K) in the Protein Data Bank. After dissociation (thermal or photoinduced) or diffusing from solution, NO can bind to a domed heme whose iron is displaced toward the proximal His. The letters (X, B, D, A) refer to the kinetic model. This scheme is applicable to other proteins studied, with time constants given in Table 1. The bimolecular rebinding, occurring in microsecond time scale, is represented as a constant term. (B) Evolution of the population of the species A, D, B, and X, according to rate equations (see *Materials and Methods*) for Mb-NO. (C) Evolution of the population ratio of the six-coordinate (species D) to five-coordinate ($B + X + \text{const}$) nonplanar species, for Mb-NO.

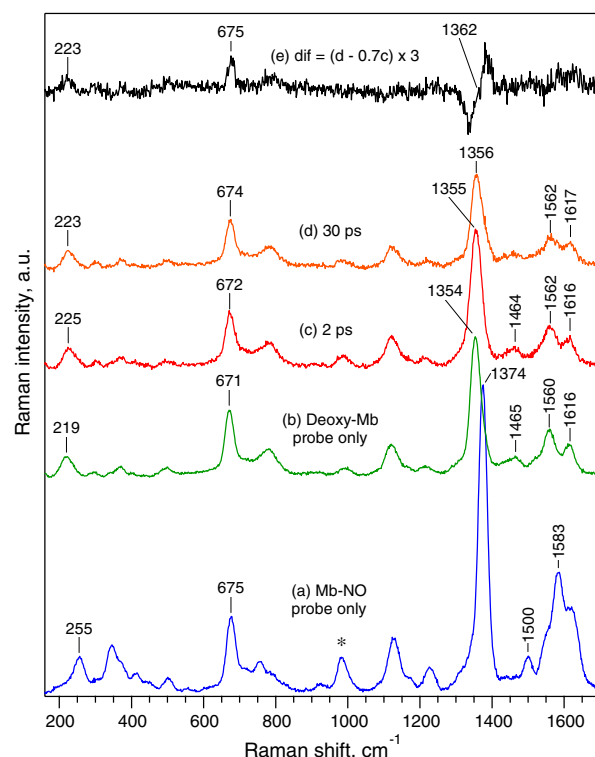


Fig. 3. TR³ spectra in the range $150\text{--}1,700 \text{ cm}^{-1}$ of Mb-NO (a, probe only), deoxy-Mb (b, probe only), Mb-NO photoproducts (species D + B + X + const) at $\Delta t = 2$ ps (c) and $\Delta t = 30$ ps (d), and the weighted difference (e) of spectrum (d) minus spectrum (c). Note that trace (e) is magnified 3 times. The asterisk indicates Raman band of SO_4^{2-} utilized for intensity normalization.

revealing slower kinetics of $\nu_{\text{Fe-His}}$ band intensity in glycerol in spite of faster geminate recombination. This is consistent with the hypothesis of a slower iron motion as increased viscosity slows down the protein fluctuations.

The difference in kinetics of TA and TR-IR (Fig. 1B) may be explained, along the same line of reasoning, by the fact that TR-IR directly probes NO coordination, whereas visible TA kinetics reflect the change in the electronic configuration of the heme, not only the Fe coordination. However, because TA in the range 400–650 nm is quite insensitive to small nonplanar porphyrin distortions (33), the effect is rather weak. We have performed TA measurements of the charge transfer Band III (755–760 nm) whose intensity was hypothesized to depend upon the Fe position and thus may reflect heme doming (34). The main observation (Fig. S4) is that the Band III kinetics comprises a phase slower than those of the background (tail of the Q bands). This latter result, as well as the simultaneous measurement of $\nu_{\text{Fe-His}}$ and ν_4 modes, supports our conclusion that the observed difference in the kinetics of iron motion and NO rebinding is not due to instrumental differences between TR³ and TA experiments, but is intrinsic to the protein. To further study the retarded domed-to-planar heme transition after NO binding, we investigated various nitrosylated proteins.

The configuration of the NO binding to the domed heme in species D could in principle be studied by detection of the kinetics of the $\nu_{\text{Fe-NO}}$ ($\sim 554 \text{ cm}^{-1}$) and $\nu_{\text{N-O}}$ ($\sim 1,613 \text{ cm}^{-1}$) stretching modes. However, such studies are as yet compromised by the

combination of (i) extremely small amplitudes, (ii) spectral congestion, in particular for $\nu_{\text{N-O}}$, (iii) the presence of similar bands in the planar six-coordinate species, which is the most populated species in the experiments at any time and whose contribution must be subtracted, and (iv) the lack of any reference spectra and a priori knowledge of these bands in domed six-coordinate heme. By contrast the $\nu_{\text{Fe-His}}$ and ν_4 Raman bands (Fig. S3) on which we focus in this study provide strong and background free markers of the heme configuration that are well suited for quantitative analysis.

Effect of Hydrogen Bonding Between Nitric Oxide and Distal Histidine.

One of the most important distal side chains is His64, which stabilizes NO (35) and which experiences a motion within 10 ps after diatomic ligand dissociation (21). To evaluate a possible role of electrostatic interaction between NO and His64 in the observed effect, we have studied the H64V Mb mutant, whose apolar Valine side chain does not interact with NO. The general behavior of $\nu_{\text{Fe-His}}$ intensity in the mutant protein (Fig. 4A and B and Table 1) was found similar to that of wild-type Mb (Fig. 1) with the same time constant $\tau_D = 30 \pm 15 \text{ ps}$, despite faster NO geminate rebinding in H64V Mb. We conclude that the domed-to-planar heme transition does not depend on the stabilizing interaction between NO and His64, which is involved only in diatomic stabilization after binding (35) and not in heme relaxation.

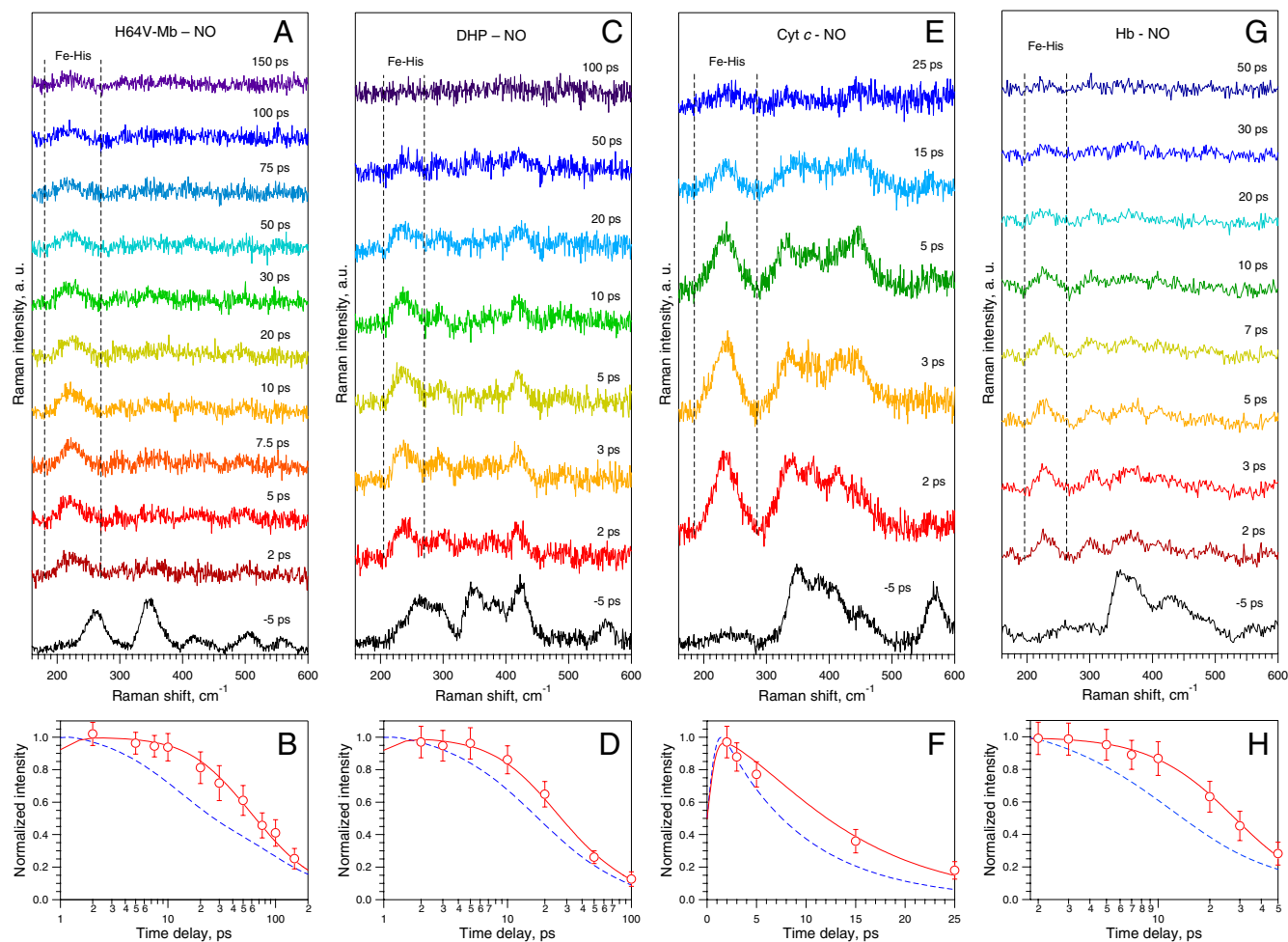


Fig. 4. TR³ spectra of various heme proteins studied and corresponding kinetics of the $\nu_{\text{Fe-His}}$ mode during NO rebinding: Mb-H64V mutant (A), DHP (C), Cyt c (E), Hb (G), and the corresponding kinetics of the mode $\nu_{\text{Fe-His}}$ (B, D, F, and H) calculated according to rate equations using time constants and yielding τ_D as in Table 1. The blue dashed curve in the lower panels represents the absorption kinetics to be compared to that of the mode $\nu_{\text{Fe-His}}$.

Effect of Sequence with the Same Globin Fold. In order to investigate the influence of the sequence in the constraints on heme iron relaxation, we similarly studied the ferrous nitrosylated DHP, an invertebrate heme protein involved in catalytic oxidation of various halophenols (36) whose fold is similar to that of Mb. This allowed us to vary the sequence, but keeping a similar tertiary globin fold. Femtosecond TA measurement of DHP revealed that NO geminate rebinding is double-exponential (Table 1 and Fig. S1), the first component being the same as in Mb, whereas the second is about two times faster. TR³ spectra and kinetics of the $\nu_{\text{Fe-His}}$ intensity after NO dissociation from DHP (Fig. 4 C and D) exhibit both similarity and differences as compared to Mb. Before photodissociation ($\Delta t = -5$ ps), the spectrum of the six-coordinate DHP-NO complex (Fig. 4C) does not show the $\nu_{\text{Fe-His}}$ stretching, which appears at 230 cm^{-1} faster than 1 ps after NO photolysis, as in Mb. The kinetics of $\nu_{\text{Fe-His}}$ intensity also deviates from expectation based on TA measurement (Fig. 4D) indicating noninstantaneous domed-to-planar heme transition. However, the fit using the model of Fig. 2 yields $\tau_{\text{D}} = 7 \pm 2$ ps for the transition toward a planar heme, which is much faster for DHP than for Mb.

Effect of Covalent Links Between Protein and Heme. In order to evaluate the influence of covalent links between protein and heme, we performed measurements on ferrous mitochondrial Cyt *c* whose heme is covalently linked to the protein. The heme iron in Cyt *c* is six-coordinated, so that the binding of NO necessitates the thermal displacement of the distal Met (28). The induced absorption corresponds to that of five-coordinate heme and the transient difference spectrum (Fig. S1) corresponds to geminate rebinding of NO. The $\nu_{\text{Fe-His}}$ stretching is absent in the spectrum of nitrosylated Cyt *c* at $\Delta t = -5$ ps (Fig. 4E) due to planarity of the six-coordinate heme and appears at 233 cm^{-1} immediately after NO photodissociation due to heme doming. The population of domed species decreases rapidly as probed by difference TR³ spectra from 2 to 25 ps (Fig. 4E) and the kinetics of the $\nu_{\text{Fe-His}}$ band intensity deviates again from that measured by TA (Fig. 4F). Contrary to Mb, NO geminate rebinding in Cyt *c* is monoexponential and fast ($\tau_1 = 8.4$ ps); solving the rate equations for a monoexponential behavior yields a relaxation time constant $\tau_{\text{D}} = 6 \pm 2$ ps, revealing less constraints on the iron through the proximal histidine than in Mb. Thus, neither the Cyt *c* rigidity due to heme-protein covalent links nor the monoexponential character of NO rebinding leads to a quasi-instantaneous (femtosecond) domed-to-planar heme transition that again occurs with a picosecond delay.

Heme Iron Relaxation in the Allosteric Protein Hemoglobin. Because the T \rightarrow R allosteric transition in hemoglobin is triggered by the iron motion toward the heme plane, we aimed at verifying whether the same behavior is observed in the tetrameric Hb. As a result of TR³ and TA measurements on Hb-NO (Fig. 4 G and H, Fig. S1E, and Table 1), we have also found the retarded $\nu_{\text{Fe-His}}$ kinetics in Hb, but with a time constant $\tau_{\text{D}} = 15 \pm 6$ ps, faster than in Mb, showing that the interaction between monomers does not increase the constraints exerted on the heme iron in the T state of Hb with respect to its homologous monomeric counterpart. The implications are discussed below.

Discussion

We report that the heme iron does not move instantaneously into the macrocycle plane after binding NO as a sixth coordination, but experiences a delayed picosecond transition from domed-to-planar heme for all proteins studied here, with the time constant depending upon the protein. This iron motion represents the very first structural event in heme proteins taking place after NO binding. This finding has several implications.

First, NO can bind to a domed five-coordinate high-spin ferrous heme. Such a possibility has been hypothesized (15) from

the absence of energy barrier for NO rebinding and agrees with theoretical calculation indicating that NO can bind to an out-of-plane iron (37). The ability to bind to a domed heme contributes to the difference in reactivity between NO and CO (SI Text), and we carried out preliminary TR³ experiments that revealed the same behavior for Mb-O₂ interaction as Mb-NO.

Second, the delayed iron motion reveals structural constraints exerted by the protein on the heme. Such constraints imply that structural changes of the heme pocket and/or its close vicinity have taken place after the dissociation of diatomics (faster than τ_{D}). A time-resolved circular dichroism (TRCD) study on Mb-CO (38) reported a motion of the proximal histidine with 7-ps time constant after CO dissociation, and a TR³ study (39), probing the aromatic Mb side chains in the heme vicinity, observed localized structural motions with 8-ps time constant. Furthermore, another TRCD study (40) has shown that the primary protein structural change after gaseous ligand release is the same for Hb-CO and Mb-CO and remarkably, for both Mb and Hb a similar “scissoring” concerted motion of the α -helices positioned on each side of the heme pocket has been observed (13, 41) during the R \rightarrow T transition. Perutz described the unliganded deoxy-Hb as a “tensed” structure, having a strain between the proximal histidine and the heme iron (9, 10), which relaxes in the liganded oxy-Hb state. The constraints in Hb were demonstrated in conditions where the Fe-His bond is broken upon diatomic binding (42). The removal of the underlying constraints in the heme vicinity during the T \rightarrow R transition, first proposed by Perutz for Hb (9), necessitates overcoming an energy barrier and thus cannot be immediate, but requires some time, causing the retardation of iron movement exactly as we observed in the present study for Hb-NO. The observed delayed motion from domed-to-planar heme ($\tau_{\text{D}} = 15$ ps) may constitute the very first step triggering the T \rightarrow R allosteric transition in hemoglobin.

An evident effect of the protein structure on the heme iron motion is revealed by the DHP versus Mb experiment. Sharing the same globin fold but different sequence, DHP experiences faster domed-to-planar heme transition than Mb (7 ps versus 30 ps). This contrasting behavior suggests less constraint in DHP and a difference in energy barrier to be overcome before iron motion. Remarkably, a photoacoustic calorimetric study found that DHP is more flexible than Mb (36). Taken together, these findings reveal the importance of side-chain interactions for the flexibility of the protein passed onto the ultrafast iron motion. It is important to note that both Mb and Hb experience concerted motions of entire helices (13, 41), whereas the peroxidase function of DHP does not require such a motion. It is also noteworthy that DHP and Cyt *c* have similar time constant τ_{D} despite their different structure and heme linking, revealing that several factors, not only the protein flexibility, can influence the heme response kinetics.

So far, it has been a commonly accepted idea that diatomic ligand binding produces an instantaneous planar heme. As our data show, this is not the case. The difference in time constant of heme structural response depending on ligand release or binding must be put in context of allostery. The quasi-instantaneous motion of heme iron upon gaseous ligand dissociation can be considered as the very primary triggering event for further conformational changes toward the equilibrium unliganded deoxy state (11). By contrast, for the reverse process of NO binding, the primary structural event of domed-to-planar heme transition takes ~ 30 ps in Mb and ~ 15 ps in Hb. Therefore, the view that in-plane motion of the heme iron following gaseous ligand binding is an instantaneous mere mechanistic event, like pulling a switch (9) whose motion is subsequently propagated through the protein structure bond after bond, should be revised. Our results support the view that ligand binding changes the protein potential energy curve (43) so that thermally driven (44, 45) fluctuations facilitate overcoming an energy barrier toward a new energy minimum, leading to the motion of the heme iron. We suggest that these con-

straints, revealed by the delayed domed-to-planar heme transition, play a crucial role in switching from one allosteric state into another in Hb and possibly also in heme-based sensors.

Materials and Methods

Time-Resolved Raman Spectroscopy. The TR³ apparatus has 0.7-ps temporal resolution and 25-cm⁻¹ spectral resolution (28, 46, 47). The broad band photolysis pulse (560–570 nm; 2 μJ; 100 fs) is delayed and collinearly superimposed to the probe beam (435 nm; 25 cm⁻¹; 25 nJ). The pure transient TR³ spectrum of photoproduct at a given time delay is obtained as described in *SI Text*. Time-resolved absorption spectroscopy and sample preparation are described in *SI Text*.

Calculation of Time Constant τ_D from the Kinetics of ν_{Fe-His} Intensity. To obtain the time constant τ_D for the transition from domed 6-c to planar 6-c heme (D → A, Fig. 2), we resolved the rate equations for population decay of all nonplanar heme species (see *SI Text*). The kinetic model employed was similar to that of ref. 15 but with the additional species domed 6c-heme (D). The set of following rate equations was solved:

$$\begin{aligned} dA/dt &= k_{DA}D(t) & dD/dt &= k_{BD}B(t) - k_{DA}D(t) \\ dB/dt &= k_{XB}X(t) - k_{BD}B(t) & dX/dt &= -k_{XB}X(t) \end{aligned} \quad [1]$$

with the total population A(t) + D(t) + B(t) + X(t) + const = 1. The only planar heme species is A(t) so that the total nonplanar population is 1 – A(t) = D(t) + B(t) + X(t) + const. The initial conditions are A(0) = 0, D(0) = 0. X(0) and B(0) are normalized amplitudes of rebinding phases after NO photodissociation (Table 1). The rate constants k_{XB} and k_{BD} were measured by transient absorption. k_{DA} = 1/τ_D is to be determined and was varied until the kinetics of the nonplanar population D(t) + B(t) + X(t) + const fits the experimental points obtained from the normalized area of the ν_{Fe-His} Raman band.

ACKNOWLEDGMENTS. We thank A. Jasaitis and S. Cianetti for their help in preparing the samples and J.M. Sintes and X. Solinas for technical assistance. S.G.K. was supported by Ecole Polytechnique and Institut National de la Santé et de la Recherche Médicale during his work at Laboratoire d'Optique et Biosciences.

- Ignarro LJ, Buga GM, Wood KS, Byrns RE, Chaudhuri G (1987) Endothelium-derived relaxing factor produced and released from artery and vein is nitric oxide. *Proc Natl Acad Sci USA* 84:9265–9269.
- Knowles RG, Palacios M, Palmer RMJ, Moncada S (1989) Formation of nitric oxide from L-arginine in the central nervous system—A transduction mechanism for stimulation of the soluble guanylate cyclase. *Proc Natl Acad Sci USA* 86:5159–5162.
- Verma A, Hirsch DJ, Glatt CE, Ronnet GV, Snyder SH (1993) Carbon monoxide—a putative neuronal messenger. *Science* 259:381–384.
- Kim HP, Ryter SW, Choi AMK (2006) CO as a cellular signaling molecule. *Annu Rev Pharmacol Toxicol* 46:411–449.
- Ghosh A, ed. (2008) *The Smallest Biomolecules: Diatomics and Their Interactions with Heme Proteins* (Elsevier, Amsterdam).
- Brunori M (2001) Nitric oxide moves myoglobin centre stage. *Trends Biochem Sci* 26:209–210.
- Brunori M, Vallone B (2006) A globin for the brain. *FASEB J* 20:2192–2197.
- Monod J, Wyman J, Changeux JP (1965) On nature of allosteric transitions—a plausible model. *J Mol Biol* 12:88–118.
- Perutz MF (1970) Stereochemistry of cooperative effects in haemoglobin. *Nature* 228:726–793.
- Perutz MF, Wilkinson AJ, Paoli M, Dodson GG (1998) The stereochemical mechanism of the cooperative effects in hemoglobin revisited. *Annu Rev Biophys Biomol Struct* 27:1–34.
- Franzen S, Lambry JC, Bohn B, Poyart C, Martin JL (1994) Direct evidence for the role of heme doming as the primary event in the cooperative transition of hemoglobin. *Nat Struct Biol* 1:230–233.
- Zhu L, Sage JT, Champion PM (1994) Observation of coherent reaction dynamics in heme-proteins. *Science* 266:629–632.
- Kachalova GS, Popov AN, Bartunik HD (1999) A steric mechanism for inhibition of CO binding to heme proteins. *Science* 284:473–476.
- Vos MH (2008) Ultrafast dynamics of ligands within heme proteins. *Biochim Biophys Acta Bioenergetics* 1777:15–31.
- Ionascu D, et al. (2005) Temperature-dependent studies of NO recombination to heme and heme proteins. *J Am Chem Soc* 127:16921–16934.
- Lim MH, Jackson TA, Anfirud PA (1997) Ultrafast rotation and trapping of carbon monoxide dissociated from myoglobin. *Nat Struct Biol* 4:209–214.
- Kim S, Jin G, Lim M (2004) Dynamics of geminate recombination of NO with myoglobin in aqueous solution probed by femtosecond mid-IR spectroscopy. *J Phys Chem B* 108:20366–20375.
- Mizutani Y, Kitagawa T (1997) Direct observation of cooling of heme upon photodissociation of carbonmonoxy myoglobin. *Science* 278:443–446.
- Findsen EW, Friedman JM, Ondrias MR, Simon SR (1985) Picosecond time resolved resonance Raman studies of hemoglobin—implications for reactivity. *Science* 229:661–665.
- Schlichting I, Berendzen J, Phillips GN, Sweet RM (1994) Crystal structure of photolyzed carbonmonoxy-myoglobin. *Nature* 371:808–812.
- Schotte F, et al. (2003) Watching a protein as it functions with 150-ps time-resolved X-ray crystallography. *Science* 300:1944–1947.
- Bourgeois D, et al. (2006) Extended subnanosecond structural dynamics of myoglobin revealed by Laue crystallography. *Proc Natl Acad Sci USA* 103:4924–4929.
- Schotte F, Soman J, Olson JS, Wulff M, Anfirud PA (2004) Picosecond time-resolved X-ray crystallography: probing protein function in real time. *J Struct Biol* 147:235–246.
- Kruglik SG, et al. (2007) Subpicosecond oxygen trapping in the heme pocket of the oxygen sensor FixL observed by time-resolved resonance Raman spectroscopy. *Proc Natl Acad Sci USA* 104:7408–7413.
- Mizutani Y, Kitagawa T (2001) Ultrafast structural relaxation of myoglobin following photodissociation of carbon monoxide probed by time-resolved resonance Raman spectroscopy. *J Phys Chem B* 105:10992–10999.
- Kitagawa T, Li X-Y (1988) Heme protein structure and the iron-histidine stretching mode. *Biological Applications of Raman Spectroscopy*, ed TG Spiro (Wiley, New York), 3, pp 97–131.
- Stavrov SS (1993) The effect of iron displacement out of the porphyrin plane on the resonance Raman spectra of heme-proteins and iron porphyrins. *Biophys J* 6:1942–1950.
- Negrerie M, Cianetti S, Vos MH, Martin JL, Kruglik SG (2006) Photoinduced coordination dynamics of cytochrome c: Ferrous versus ferric species studied by time-resolved resonance Raman and transient absorption spectroscopies. *J Phys Chem B* 110:12766–12781.
- Negrerie M, et al. (2006) Role of heme iron coordination and protein structure in the dynamics and geminate rebinding of nitric oxide to H93G myoglobin: Implications for NO-sensors. *J Biol Chem* 281:10389–10398.
- Ye X, et al. (2003) Investigations of heme protein absorption line shapes, vibrational relaxation, and resonance Raman scattering on ultrafast time scales. *J Phys Chem A* 107:8156–8165.
- Spiro TG (1988) Resonance Raman spectroscopy of metalloporphyrins. *Biological Applications of Raman Spectroscopy*, ed TG Spiro (Wiley, New York), 3, pp 1–37.
- Shreve AP, Franzen S, Simpson MC, Dyer RB (1999) Dependence of NO recombination dynamics in horse myoglobin on solution glycerol content. *J Phys Chem B* 103:7969–7975.
- Haddad RE, et al. (2003) Origin of the red shifts in the optical absorption bands of nonplanar tetraalkylporphyrins. *J Am Chem Soc* 125:1253–1268.
- Stavrov SS (2001) Optical absorption band III of deoxyheme proteins as a probe of their structure and dynamics. *Chem Phys* 271:145–154.
- Olson JS, Phillips GN (1997) Myoglobin discriminates between O₂, NO, and CO by electrostatic interactions with the bound ligand. *J Biol Inorg Chem* 2:544–552.
- Miksovskaja J, Horsa S, Davis MF, Franzen S (2008) Conformational dynamics associated with photodissociation of CO from dehaloperoxidase studied using photoaoustic calorimetry. *Biochemistry* 47:11510–11517.
- Franzen S (2002) Spin-dependent mechanism for diatomic ligand binding to heme. *Proc Natl Acad Sci USA* 99:16754–16759.
- Dartigalongue T, Hache F (2005) Observation of sub-100 ps conformational changes in photolyzed carbonmonoxy-myoglobin probed by time-resolved circular dichroism. *Chem Phys Lett* 415:313–316.
- Sato A, Gao Y, Kitagawa T, Mizutani Y (2007) Primary protein response after ligand photodissociation in carbonmonoxy myoglobin. *Proc Natl Acad Sci USA* 104:9627–9632.
- Dartigalongue T (2005) Conformational dynamics of myoglobin studied by time-resolved circular dichroism. PhD thesis (Ecole Polytechnique, Palaiseau, France).
- Rodgers KR, Spiro TG (1994) Nanosecond dynamics of the R → T transition in hemoglobin: Ultraviolet Raman studies. *Science* 265:1697–1699.
- Paoli M, Dodson G, Liddington RC, Wilkinson AJ (1997) Tension in haemoglobin revealed by Fe-His(F8) bond rupture in the fully liganded T-state. *J Mol Biol* 271:161–167.
- Goodey NM, Benkovic SJ (2008) Allosteric regulation and catalysis emerge via a common route. *Nat Chem Biol* 4:474–482.
- Armstrong MR, Ogilvie JP, Cowan ML, Miller RJD (2003) Observation of the cascaded atomic-to-global length scales driving protein motion. *Proc Natl Acad Sci USA* 100:4990–4994.
- Popovych N, Sun S, Ebricht RH, Kalodimos CG (2006) Dynamically driven protein allostery. *Nat Struct Mol Biol* 13:831–838.
- Kruglik SG, et al. (2007) Molecular basis for nitric oxide dynamics and affinity with *Alcaligenes xylosoxidans* cytochrome c'. *J Biol Chem* 282:5053–5062.
- Kruglik SG, Lambry J-C, Martin J-L, Vos MH, Negrerie M (2010) Sub-picosecond Raman spectrometry for time-resolved studies of structural dynamics in heme proteins. *J Raman Spectrosc* doi:10.1002/jrs.2685.